IEEE Access
Multidisciplinary ⋮ Rapid Review ⋮ Open Access Journal

Received August 25, 2020, accepted September 7, 2020, date of publication September 11, 2020,
date of current version September 24, 2020.

Digital Object Identifier 10.1109/ACCESS.2020.3023457

A Joint Optimization Algorithm Using Adaptive Minimum Coset Number Based Discrete Multi-Coset Sampling

JIANNAN DONG, HONGKUN LI, ZHENFANG FAN, QIANG ZHOU, AND SHUNGANG HUA
School of Mechanical Engineering, Dalian University of Technology, Dalian 116024, China

Corresponding author: Hongkun Li (lihk@dlut.edu.cn)

This work was supported in part by the Natural Science Foundation of China under Grant U1808214, and in part by the Fundamental Research Funds for the Dalian University of Technology under Grant DUT20LAB125.

ABSTRACT We address the problem of sparse multi-band signal reconstruction in the case of unknown band position through the discrete multi-coset sampling (DMCS). In this article, the signal has complex frequency components, and the minimum coset number is determined on the assumption that there is only one frequency component with same characteristics. According to the frequency characteristics, we analyze the influence of the parameterized compressed matrix on the two reconstruction algorithms, and get that a single algorithm does not have universal adaptability to different frequency components. In order to solve this problem, under the discrete multi-coset sampling model, a joint optimization algorithm with discriminant factor (DF-JOA) is proposed to identify the different characteristics and automatically select an appropriate algorithm for signal reconstruction, numerical simulation experiments show the effectiveness of the algorithm. We also simulate the reconstruction success ratio of amplitude and the total coset number under different compressed matrices, determine the influence law, and confirm the improvement of signal reconstruction probability by joint optimization algorithm. Our method ensures the spectrum reconstruction of the multi-band signal. This article can guide how to better select the coset parameters under the condition that the channels of the discrete multi-coset sampling system are limited but the minimum coset number can be guaranteed. It will have a great significance to the sub-Nyquist sampling technique.

INDEX TERMS Discrete multi-coset sampling, sparse reconstruction, minimum coset number, discriminant factor, joint optimization algorithm.

I. INTRODUCTION

The signal is the carrier of the message and the tool to carry the message, the sampling of the signal is the basic way to obtain the signal information. At the beginning of the 20th century, Whittaker [1], Nyquist [2], Kotel'nikov [3], and Shannon [4] made a great contribution to the field of signal sampling theory and laid the foundation. It requires that the sampling rate is not less than two times the highest frequency of the signal. People also have never stopped studying the sampling theory [5]–[7]. With the rapid development of many fields (such as bandwidth communication and radio frequency technology), narrowband signals are modulated to a very high frequency spectrum. That make it more and more difficult for sampling frequency to meet the requirements of sampling theory [8], and even exceed the capability of analog-to-digital converter (ADC) to a great extent. The maximum sampling rate of ADC is affected by materials and technology, so it has become a difficult problem in the field of signal processing.

In the late 1960s, people began to study the sub-Nyquist sampling of multi-band signals. In 1967, Landau [9] proposed that the minimum sampling rate of a spectral sparse signals in the sum of the bandwidths of all subbands, which is lower than the corresponding Nyquist rate. Under this condition, the original signal can be reconstructed perfectly. In 1977, Papoulis [10] conducted the theory of non-uniform sampling. Then Venkataramani and Bresler [11] proposed a periodic non-uniform sub-Nyquist sampling technique called multi-coset sampling, and effectively used it to reduce the

The associate editor coordinating the review of this manuscript and approving it for publication was Jinming Wen.

sampling rate of multi-band signal in [12]–[14]. Similarly, Mishali and Eldar [15], [16] raised a modulated wideband converter model for multi-channel sub-Nyquist sensing, and derived the minimum sampling rate that can accurately recover the signal. Unlike the former, it is a uniform sampling system. In 2006, a new sampling concept, ''compressive sensing (CS)'', proposed by Candès *et al.* [17], Donoho [18], and Candès and Wakin [19]. Compared with the Shannon-Nyquist sampling theorem, CS is not limited by the signal bandwidth, but makes use of the sparsity of the signal. For example, some real signals are sparse in some transform domains [20], [21].

With the addition of the concept of compressive sensing, it is well introduced the research of sub-Nyquist sampling technology. Tian and Giannakis [22] introduced CS to wideband spectrum sensing, using sub-Nyquist rate samples to detect and classify multi-band signals through wavelet-based edge detectors. Fleyer *et al.* [23] adopted the structure of multi-rate synchronous sampling and used the reconstruction algorithm of compressive sensing to solve the underdetermined equations. In [13], [24], [25], multi-coset sampling was applied to the field of blind power spectrum sampling. With the help of compressive sensing, the power spectrum estimation of the signal at a rate lower than that of Nyquist sampling is realized, and there is no limitation of sparsity and no need to reconstruct the signal.

At present, the spectrum reconstruction for sub-Nyquist sampling is still in the research stage, many algorithms have been applied to spectrum sensing, and achieved good results. However, there is still a lot of work to be done on the algorithm research of different frequency characteristics and the influence of compressed matrix on the signal reconstruction.

The rest of the article will carry on the related work, and is organized as follows. In section II, the mathematical model of discrete multi-coset sampling is established, and the structural parameters of the system are determined. Based on the theoretical model, section III introduces the core idea of signal reconstruction and the research basis of establishing the minimum coset number as the text. According to the analysis of two algorithms in section IV, a joint optimization algorithm with discriminant factor is proposed in section V to adaptively identify frequency features for signal spectrum reconstruction. In section VI, we get the influence of frequency amplitude and total coset number on signal reconstruction under different compressed matrices. Finally, the conclusions are given in section VII.

II. DISCRETE MULTI-COSET SAMPLING

The Nyquist sampling technique samples discretely the time continuous signal $x(t)$ at a fixed time interval T to obtain the sampling sequence $x[m] = x(mT)$ for $m = 0, 1, \ldots, M-1$. Discrete multi-coset sampling is a multi-channel discrete periodic non-uniform sub-Nyquist sampling technique [25], [26], the structural framework and schematic diagram of the sampling system is shown in Fig.1. It samples $x(t)$ at $t = (nL + c_i)T$ for $i = 1, 2, \ldots, p$ and

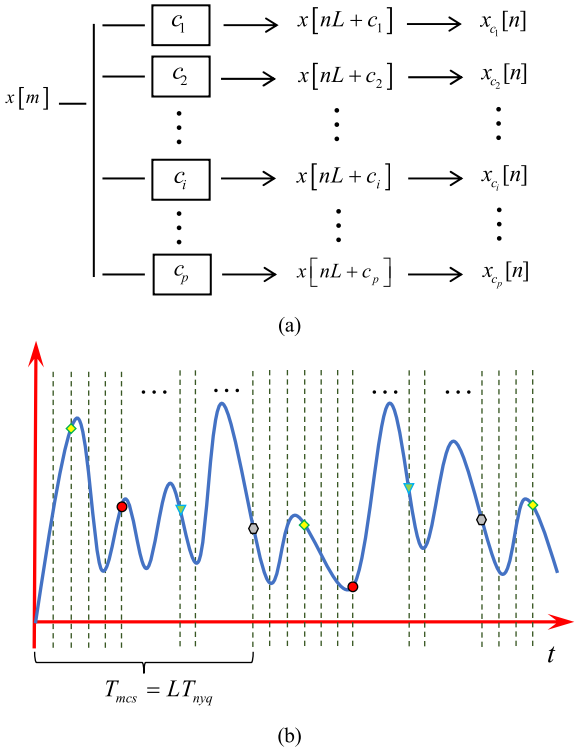

FIGURE 1. (a) is the framework and (b) is the schematic diagram of the discrete multi-coset sampling system.

$n = 0, 1, \ldots, N-1$, where the total coset number L is positive integer, the fixed time interval LT is greater than or equal to the Nyquist sampling period T, p is the number of channels required by the multi-coset sampling system, the offset c_i satisfies $0 \le c_1 < \cdots < c_i < \cdots < c_p \le L-1$. The channel samples the signal at the rate $1/(LT)$ Hz after the sampling offset $c_i T$. L, c_i, and p constitute the structural parameters of the sampling system. Then the sampling sequence of the i-th channel can be listed as:

$$x_{c_i}[n] = x[nL + c_i] \tag{1}$$

where $n = 0, 1, 2, \ldots, N-1$.

According to Fig.1 and Eq. (1), the discrete multi-coset sampling sequence is a partial sequence dominated by c_i variables in the Nyquist sampling sequence, where $m = nL + c_i$, $M = NL$.

The discrete Fourier transform (DFT) of the Nyquist sequence is as follows:

$$Y[k] = \sum_{m=0}^{M-1} x[m] \exp(-j \cdot 2\pi mk/M) \tag{2}$$

where $k = 0, 1, 2, \ldots, M-1$.

Similarly, the DFT of the sampling sequence of the i-th channel of the multi-coset sampling is:

$$y_i[k_c] = \sum_{n=0}^{N-1} x_{c_i}[n] \exp(-j \cdot 2\pi nk_c/N) \tag{3}$$

where $k_c = 0, 1, 2, \ldots, N-1$.

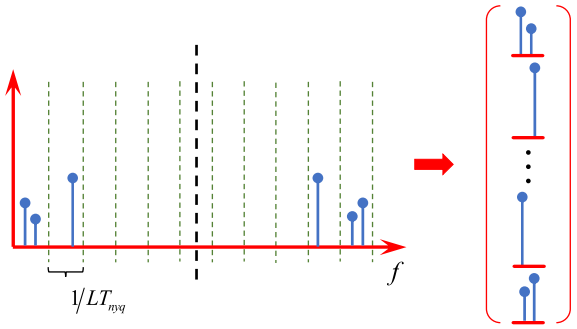

FIGURE 2. Schematic diagram of spectrum division.

We can sort out the results of M-term Fourier transform of the Nyquist sampling sequence into a matrix $\mathbf{Y}_{\mathrm{L}}$ (spectrum division matrix) with the size of $L \times N$. The entire frequency band is divided into L subbands (the row vector of matrix $\mathbf{Y}_{\mathrm{L}}$) as shown in Fig.2. Its subband Y_l for $l = 1, 2, \ldots L$ is:

$$Y_l = [Y[(l-1)N], Y[(l-1)N+1], \ldots Y[(l-1)N+N-1]] \quad (4)$$

where the size of Y_l is $1 \times N$.

So, the spectrum division matrix $\mathbf{Y}_{\mathrm{L}}$ can be expressed as:

$$\mathbf{Y}_{\mathrm{L}} = [Y_1, Y_2, \ldots, Y_l, \ldots, Y_L]^{\mathrm{T}} \quad (5)$$

The column vector $Y_{\mathrm{L}}(k_c)$ for $k_c = 0, 1, 2, \ldots, N-1$ of the spectrum division matrix $\mathbf{Y}_{\mathrm{L}}$ is:

$$Y_{\mathrm{L}}(k_c) = [Y[k_c], Y[N+k_c], \ldots, Y[(l-1)N+k_c], \ldots, Y[(L-1)N+k_c]]^{\mathrm{T}} \quad (6)$$

where the size of $Y_{\mathrm{L}}(k_c)$ is $L \times 1$.

We define the compressed matrix $\mathbf{A}$ with the size of $p \times L$, its element is $\alpha_{i,l} = \exp(j \cdot 2\pi c_i (l-1)/)$. Its row vector is recorded as α_i for $i = 1, 2, \ldots, p$. Then, the vector α_i is multiplied by the vector $Y_{\mathrm{L}}(k_c)$, we have

$$\begin{aligned}
\alpha_i Y_{\mathrm{L}}(k_c) &= \sum_{l=1}^{L} \alpha_{i,l} Y[(l-1)N + k_c] \\
&= \sum_{l=1}^{L} \exp(j \cdot 2\pi c_i (l-1)/L) \\
&\quad \times \sum_{m=0}^{M-1} x[m] \exp(-j \cdot 2\pi m((l-1)N + k_c)/M) \\
&= \sum_{m=0}^{M-1} x[m] \sum_{l=1}^{L} \exp(-j \cdot 2\pi ((m - c_i)(l-1)N \\
&\quad + m k_c)/M) \\
&= L \cdot \exp(-j \cdot 2\pi c_i k_c / M) \\
&\quad \cdot \sum_{n=0}^{N-1} x_{c_i}[n] \exp(-j \cdot 2\pi n k_c / N) \\
&= L \cdot \exp(-j \cdot 2\pi c_i k_c / M) \cdot y_i[k_c] \quad (7)
\end{aligned}$$

According Eq. (3), the results of N-term Fourier transform of the i-th channel can form a row vector y_i, and then p row vectors form a matrix $\mathbf{Y}_{\mathrm{c}}$ (multi-coset sampling spectrum matrix) of $p \times N$ dimension. So, the matrix $\mathbf{Y}_{\mathrm{c}}$ can be expressed as:

$$\mathbf{Y}_{\mathrm{c}} = [y_1, \ldots, y_i, \ldots, y_p]^{\mathrm{T}} \quad (8)$$

Through Eq. (4)-(8), we can get

$$\mathbf{Y}_{\mathrm{DMCS}} = \mathbf{A}\mathbf{Y}_{\mathrm{L}} \quad (9)$$

where $\mathbf{Y}_{\mathrm{DMCS}} = \mathrm{L} \cdot \mathbf{Y}_{\mathrm{c}} \circ \mathbf{B}$, $\mathbf{B}$ is the compensation matrix of $\mathbf{Y}_{\mathrm{c}}$, its element is $\beta_{i,k_c} = \exp(-j \cdot 2\pi c_i k_c / M)$, and its size is also $p \times N$, $\circ$ denotes Hadamard product (corresponding element multiplication).

Combining what has been discussed above, the discrete multi-coset sampling mathematical model is established based on the DFT of original signal Nyquist sampling sequence and the DFT of the discrete multi-coset sampling sequence. It obtains different sampling sequence by adjusting the sampling time interval and the time offset on each channel. The output sequences on each channel are mapped to the frequency domain to realize the spectrum cutting and compression conversion of the original signal.

Discrete multi-coset sampling can be divided into the following steps:

(1) Determine the structural parameters L, c_i, p of the system.

(2) Each channel samples N points.

(3) Transform the multi-coset sampling sequence by DFT, and then multiplied the compensation coefficient.

It can be seen from the mathematical model of discrete multi-coset sampling, its single channel sampling frequency $f = 1/(LT)$ Hz, frequency range $[0, f/2)$, is less than or equal to Nyquist sampling frequency $F = 1/T$ Hz, frequency range $[0, F/2)$. It can be concluded that $F = Lf$. According to Nyquist sampling theorem, the maximum frequency $f_{\max}$ of the original signal should satisfy $f_{\max} < F/2$, namely $L > 2f_{\max}/f$.

We do not know the exact value of the maximum frequency in the original signal, but we should obtain effective information from other relevant information of the signal as a prior knowledge to determine the estimated value of the range of the maximum frequency. It will be convenient for us to determine the structural parameters L and c_i of the system.

If $f_{\max} \gg f$ will make the total coset number $L \gg 1$. At this time, the spectrum characteristic of the multi-coset sampled signal belongs to the serious undersampled signal, so it is impossible to obtain the accurate information of the high-frequency signal. We need to reconstruct the spectral feature of the original signal from the multi-coset sampled undersampled signal.

III. SIGNAL RECONSTRUCTION AND MINIMUM COSET NUMBER

A. SIGNAL RECONSTRUCTION OF DISCTETE MULTI-COSET SAMPLING

Compressive sensing theory points out that if the signal is sparse or sparse in a certain transform domain,

the high-dimensional sparse signal can be projected into a low-dimensional space by an observation matrix independent of the transform domain. Then by solving an optimization problem, the original signal can be reconstructed with high probability from these few projections, and such a low-dimensional signal contains enough information of the original signal.

DFT is a classical sparse method, which transforms the non-sparse Nyquist sampling sequence $x[m]$ into sparse sequence $Y[k]$. The spectrum division matrix $\mathbf{Y}_{\mathrm{L}}$ is sparse matrix, and the column vector $Y_{\mathrm{L}}(k_c)$ of matrix is sparse vector. According to the Eq. (9), the column vector $Y_{\mathrm{DMCS}}(k_c)$ of the matrix $\mathbf{Y}_{\mathrm{DMCS}}$ is the low-dimensional vector formed by the projection of the high-dimensional sparse vector $Y_{\mathrm{L}}(k_c)$ by the compressed matrix $\mathbf{A}$.

In the discrete multi-coset sampling system, we can take the undersampled spectrum information of the discrete multi-coset sampling sequence as the system output data under the condition that the system parameters are known. And then, according to the compressive sensing theory, the spectral information of the original signal Nyquist sampling sequence is reconstructed by solving the optimization problem. Its reconstruction system framework diagram is shown in Fig.3.

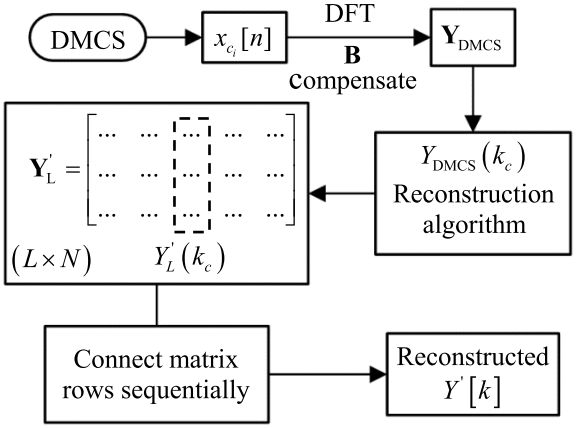

FIGURE 3. Reconstruction system framework diagram.

B. MINIMUN COSET NUMBER

In the blind sampling process of discrete multi-coset sampling, we know that the vector is a sparse vector, and there are only a few non-zero values in each vector, but we do not know its position accurately. As mentioned in the [27], [28], it is assumed that the vector $\bar{\mathbf{x}}$ is a solution of $\mathbf{y} = \mathbf{Ax}$, and define the sparsity $K = \|\mathbf{x}\|_0$, if $K \leq \mathrm{rank}(\mathbf{A})/2$ ($\mathrm{rank}(\mathbf{A})$ is the rank of the compressed matrix $\mathbf{A}$), then $\bar{\mathbf{x}}$ is the unique sparsest solution of the equation.

The spectrum division matrix $\mathbf{Y}_{\mathrm{L}}$ is formed by the results of the DFT of the Nyquist sampling sequence of original signal. There is at least one frequency in the signal, so $K = \|Y_{\mathrm{L}}(k_c)\|_0 \geq 1$. In order to meet the above requirement of the unique sparsest solution, we should make $\mathrm{rank}(\mathbf{A}) \geq 2$, that is, the number of channels of the discrete multi-coset sampling system is $p \geq 2$.

According to Eq. (2) and Euler theorem, there is a conjugate relationship between the values of spectrum information after DFT. For example, there is a frequency f_0 in the signal. After the transformation, it forms two spectral values $Y[k_{f_0}]$ and $Y[M - k_{f_0}]$, and there is a conjugate relationship between them. It can be expressed as:

$$Y[k_{f_o}] = \mathbf{conj}(Y[M - k_{f_o}]) \tag{10}$$

where $\mathbf{conj}(\cdot)$ means to conjugate the element.

So, there are two special cases for the spectrum division matrix $\mathbf{Y}_{\mathrm{L}}$:

(1) There is a multiple relation $f_0 = nf$ between the frequency f_0 of the original signal and the discrete multi-coset sampling frequency f. That will put $Y[k_{f_0}]$ and $Y[M - k_{f_0}]$ in the same column vector of the spectrum division matrix $\mathbf{Y}_{\mathrm{L}}$. Their positions in the vector have

$$\mathbf{pos}(Y[k_{f_o}]) + \mathbf{pos}(Y[M - k_{f_o}]) = L + 2 \tag{11}$$

where $\mathbf{pos}(\cdot)$ denotes the position number of the element in the vector.

At this time, $K = \|Y_{\mathrm{L}}(k_c)\|_0 \geq 2$, the number of channels of sampling system should satisfy $p \geq 4$.

(2) There are multiple frequencies in the original signal. They are only general frequencies and there is no multiple relation to the sampling frequency f mentioned in the first case. For a certain frequency f_i, we have

$$\mathbf{pos}(Y[k_{f_i}]) + \mathbf{pos}(Y[M - k_{f_i}]) = L + 1 \tag{12}$$

If there is a special relationship $f_i = f_j + nf$ (f_i and f_j are two of the frequencies), this will make at least two of $Y[k_{f_1}]$, $Y[k_{f_2}]$, …, $Y[M - k_{f_2}]$, $Y[M - k_{f_1}]$ in the same column vector. However, there is no fixed relationship between the positions of elements in the same vector.

Similarly, the number of channels of sampling system should satisfy $p \geq 4$.

In both cases, it is possible to place several different non-zero values in the same column vector. We can get, the greater the sparsity K, the more the minimum number of channels needed to reconstruct the signal.

What is studied in this article is the minimum number of channels for the reconstruction of the original signal by the discrete multi-coset sampling system, namely $p = 4$.

IV. RECONSTRUCTION ALGORITHMS AND EXISTING PROBLEMS

A. THE CONSTRAINTS OF COMPRESSED MATRIX

For the traditional compressive sensing measurement matrix, the linear independence of the measurement matrix is proposed in the [29] and the Spark theorem is proposed in the [30]. They are the basic guarantee that the compression vector can be recovered by the reconstruction algorithm, and they are also the important theoretical basis for designing the measurement matrix.

However, in the discrete multi-coset sampling model, the compressed matrix $\mathbf{A}$ cannot be designed subjectively, but a matrix with a certain pattern based on the structural parameters L, c_i, p of the periodic non-uniform sampling.

The linear independence of the matrix means that there is no correlation between the atoms. The atoms need to be linearly independent with a low coefficient of mutual coherence, so that the original signal can be reconstructed with high probability. The mutual coherence of atoms is the absolute value of the normalized inner product between different atoms, and the atomic mutual coherence coefficient of matrix $\mathbf{A}$ is expressed as:

$$\delta\left(A_{i,j}\right) = \frac{\left|a_i^{\Gamma} a_j\right|}{\|a_i\|_2 \left\|a_j\right\|_2} \tag{13}$$

where $1 \leq i, j \leq L$, and $i \neq j$, a_i is the i-th column of $\mathbf{A}$.

In the compressed matrix $\mathbf{A}$ of the discrete multi-coset sampling model, due to the characteristics of element $\alpha_{i,l}$, there are many atoms with high mutual coherence coefficient. For example, there are structural parameters such as $L = 21$, $p = 4$, $c_i = \{0, 3, 6, 8\}$. There is such a relationship as $\delta\left(A_{6,13}\right) = \delta\left(A_{6,20}\right) = \delta\left(A_{13,20}\right) = 1$, it means that the atoms are equal. And another situation is that the coefficient of mutual coherence is also relatively high, which is 0.5617 such as $\delta\left(A_{2,15}\right)$. These situations cannot satisfy the linear independence of matrix atoms, so that the signal cannot be accurately reconstructed.

The Spark constant is defined as the minimum number of linearly related columns of the matrix. The Spark theorem for sparse reconstruction is: For any vector $\mathbf{y} \in \mathrm{R}^{\mathrm{m}}$, if and only if $\mathrm{Spark}(\mathbf{A}) > 2K$, there is at most one signal $\|\mathbf{x}\|_0 = K$ that makes $\mathbf{y} = \mathbf{A}\mathbf{x}$. For the compressed matrix $\mathbf{A}$ in the model, its fixed pattern cannot fully satisfy the theorem. As shown in the example above, $a_6 = a_{13}$, makes $\mathrm{Spark}(\mathbf{A}) = 2$. In this case, sparsity $K < 1$, obviously cannot meet the requirement of reconstructing.

B. ORTHOGONAL MATCHING PURSUIT ALGORITHM

1) DETAILED INTRODUCTION OF THE ALGORITHM

For the basic equation $\mathbf{y} = \mathbf{A}\mathbf{x}$ of compressive sensing, mathematically, it is to solve the underdetermined equation under certain conditions. The reconstruction algorithms of compressive sensing can be divided into two categories: convex optimization algorithm and greedy algorithm. Convex optimization algorithm is more accurate than greedy algorithm, but requires higher computational complexity.

Therefore, greedy algorithm is widely used at present, which realizes the approximation of signal vector by selecting appropriate atoms and through a series of gradual increasing methods [31]. The orthogonal matching pursuit (OMP) algorithm which is common in greedy algorithm is applied in this article [32]–[34].

The flow of OMP algorithm:

Input: Compressed matrix $\mathbf{A}(M \times N, M \ll N)$, projection vector y $(M \times 1)$, signal sparsity K.

Output: The K-sparse approximation $\hat{\theta}$ of the target signal.

In the following process, r_t denotes the residual error, t denotes the number of iterations, $\emptyset$ denotes empty set, Λ_t denotes the index set of column ordinal numbers for t iterations, λ_t denotes index of the column serial number obtained by the t-th iteration, a_j denotes the j-th column of the matrix $\mathbf{A}$, $\mathbf{A}_t$ (matrix of size $M \times t$) denotes the set of column vectors of the matrix $\mathbf{A}$ selected by the index Λ_t, Γ denotes transpose when matrix or vector is real and conjugate transpose when complex, θ_t is the column vector of size $t \times 1$.

(1) Initialize: $r_0 = y$, $\Lambda_t = \emptyset$, $\mathbf{A}_0 = \emptyset$, $t = 1$, $\hat{\theta}$ is a zero vector of $N \times 1$ dimension.

(2) Calculate $\lambda_t = \arg \max_{j=1,2,\ldots,N} \left|r_{t-1}^{\Gamma} a_j\right|$, get the index of the column serial number λ_t.

(3) Make $\Lambda_t = \Lambda_{t-1} \cup \lambda_t$, $\mathbf{A}_t = \mathbf{A}_{t-1} \cup a_{\lambda_t}$.

(4) Calculate the least square solution of $y = \mathbf{A}_t\theta_t$:

$$\hat{\theta}_t = \arg\min_{\theta_t} \|y - \mathbf{A}_t\theta_t\| = \left(\mathbf{A}_t^{\Gamma}\mathbf{A}_t\right)^{-1}\mathbf{A}_t^{\Gamma} y.$$

(5) Update residual error:

$$r_t = y - \mathbf{A}_t\hat{\theta}_t = y - \mathbf{A}_t\left(\mathbf{A}_t^{\Gamma}\mathbf{A}_t\right)^{-1}\mathbf{A}_t^{\Gamma} y.$$

(6) $t = t + 1$, if $t \leq K$ return to step (2) to continue the iteration, otherwise, stop the iteration and proceed to step (7).

(7) Reconstruct the non-zero term of $\hat{\theta}$ at the index set Λ_t position until the final iteration of $\hat{\theta}_t$.

In the above algorithm flow, it is important to note that:

(1) In step (2), the main principle is to make use of the different contribution of the non-zero terms of the sparse vector in the compressed process. Then we calculate the maximum value of the absolute value of the inner product between the atom of the compressed matrix and the residual vector to find the suitable atom and determine the location of the non-zero term.

(2) As can be seen from step (6), the number of iterations of the algorithm is the sparsity K of the signal.

(3) In step (4), $\mathbf{A}_t^{\Gamma}\mathbf{A}_t$ is a square matrix of order t. In order to satisfy the existence of $\left(\mathbf{A}_t^{\Gamma}A_t\right)^{-1}$, its rank should be t. It means that the column vector selected in the compressed matrix should satisfy rank $\left(\mathbf{A}_t^{\Gamma}\mathbf{A}_t\right) = t$, and after the K-th iteration, rank $\left(\mathbf{A}_K^{\Gamma}\mathbf{A}_K\right) = K$.

2) PROBLEMS OF THE MODEL IN THE PROCESS OF RECONSTRUCTION

In step (2) of the OMP algorithm, the appropriate atom is selected each time according to the inner product value, and the location of the non-zero term in the sparse is determined.

For the first case of the spectrum division matrix $\mathbf{Y}_{\mathrm{L}}$, if the position number of the non-zero term $Y\left[k_{f_o}\right]$ in the sparse vector is l_{f_0}, then according to the Eq. (11) the position number of $Y\left[M - k_{f_o}\right]$ is $L + 2 - l_{f_0}$. Obviously, the elements $\alpha_{i,l_{f_0}}$ and $\alpha_{i,L+2-l_{f_0}}$ in the compressed matrix corresponding to the non-zero terms also have a conjugate relationship. In the process of compression, we can get

$$\alpha_{i,l_{f_0}} Y\left[k_{f_o}\right] = \mathbf{conj}\left(\alpha_{i,L+2-l_{f_0}} Y\left[M - k_{f_o}\right]\right) \tag{14}$$

This will make them have the same contribution to the projection vector.

When we use the projection vector for reconstruction, after the absolute value of the inner product of each atom and the projection vector is calculated in the first iteration, the results of the two atoms are equal. The OMP algorithm will select one of them as the result of the first iteration. If do this, after the residual is updated, the contribution of the other non-zero term will be weakened when the inner product value is calculated again. It is unable to select the atom effectively and determine its position, so that the atomic index obtained after the final iteration is not accurate. As a result, the reconstruction of the sparse vector is invalid.

3) SIMULATION ANALYSIS

The function of the original signal with time variable is $x(t) = \sum_{i=1}^{q} a_i \cos(2\pi f_i t) + w(t)$, $w(t)$ is the signal noise. There is a frequency $f_1 = 593.1$ Hz in the original signal, and its amplitude is $a_1 = 9.34$.

The discrete multi-coset sampling frequency is $f = 65.9$ Hz, and the coset number is $p = 4$. During the sampling process, the signal-to-noise ratio of each channel is SNR $= 3$ dB. In order to meet the requirements of reconstructed signal, we set structural parameters $L = 21$ and $c_i = \{0, 6, 14, 19\}$. Then each channel carries out the discrete sampling $N = 102400$ points.

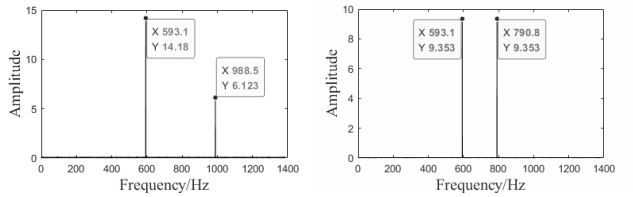

FIGURE 4. (a) is the reconstructed spectrum diagram and (b) is the original signal spectrum diagram.

According to Fig.3 and the OMP algorithm flow, we can get the reconstructed spectrum division matrix $\mathbf{Y}'_{\mathrm{L}}$ and spectral value $Y'[k]$. The reconstructed spectrum diagram is draw according to $Y'[k]$, as shown in Fig.4a. The reconstructed frequencies are 593.1Hz and 988.5Hz. In the $\mathbf{Y}'_{\mathrm{L}}$, we have $\mathbf{pos}(Y[k_{593.1}]) = 10$ and $\mathbf{pos}(Y[k_{988.5}]) = 16$, they do not satisfy the Eq. (11). This signal reconstruction is invalid.

Compared with the discrete multi-coset sampling, we perform the Nyquist sampling on the original signal. Its sampling frequency is $F = Lf = 1383.9$ Hz, and sampling points is $M = NL = 2150400$. We can get the spectral value $Y[k]$ and the spectrum diagram is shown in Fig.4b. The frequency values are 593.1Hz and 790.8Hz. In the $\mathbf{Y}_{\mathrm{L}}$, we have $\mathbf{pos}(Y[k_{593.1}]) = 10$ and $\mathbf{pos}(Y[k_{790.8}]) = 13$, which satisfy the Eq. (11).

Comparing the two results, it is found that the frequency 790.8Hz moves to 988.5Hz after reconstruction, and the amplitude has a large error. This is because the two non-zero terms of the frequency $f_1 = 593.1$ Hz are in the same column vector Y_{L} ($k_c = 0$) of $\mathbf{Y}_{\mathrm{L}}$. When we reconstruct the vector Y_{DMCS} ($k_c = 0$), after calculating the absolute value of inner product, $\left|r_0^{\Gamma} a_{10}\right| = \left|r_0^{\Gamma} a_{13}\right|$ appears. The algorithm selects the 10th column atom for subsequent calculation, and updates the residual error. In next iteration, this weakens the contribution of the 13th column atom corresponding to another non-zero term. Their positions in the sparse vector cannot be found accurately, resulting in reconstruction failure.

C. COMPRESSIVE SAMPLING MATCHING PURSUIT ALGORITHM

1) DETAILED INTRODUCTION OF THE ALGORITHM

Compressive sampling matching pursuit (CoSaMP) algorithm is an influential reconstruction algorithm proposed by D. Needell [35], and it is also an improvement of OMP algorithm. In each iteration, multiple atoms are selected to gradually increase to achieve signal vector approximation.

The flow of CoSaMP algorithm:

Input: Compressed matrix $\mathbf{A}(M \times N, M \ll N)$, projection vector y $(M \times 1)$, signal sparsity K.

Output: The K-sparse approximation $\hat{\theta}$ of the target signal.

In the following process, r_t denotes the residual error, t denotes the number of iterations, $\emptyset$ denotes empty set, J_0 denotes the column index number found in each iteration, Λ_t denotes the index set of column ordinal numbers for t iterations, a_j denotes the j-th column of the matrix $\mathbf{A}$, $\mathbf{A}_t$ denotes the set of column vectors of the matrix $\mathbf{A}$ selected by the index Λ_t, Γ denotes transpose when matrix or vector is real and conjugate transpose when complex.

(1) Initialize: $r_0 = y$, $\Lambda_t = \emptyset$, $\mathbf{A}_0 = \emptyset$, $t = 1$, $\hat{\theta}$ is a zero vector of $N \times 1$ dimension.

(2) Calculate $u_j = \left|r_{t-1}^{\Gamma} a_j\right|$ for $j = 1, 2, \ldots, N$, and put all the u_j into the set U. Then select $2K$ maximum values from U, and make the column number j of matrix $\mathbf{A}$ corresponding to these values to form the column number set J_0.

(3) Make $\Lambda_t = \Lambda_{t-1} \cup J_0$, $\mathbf{A}_t = \mathbf{A}_{t-1} \cup a_j$ (for all $j \in J_0$), if the number of columns of $\mathbf{A}_t$ is greater than the number of rows, exit the process.

(4) Calculate the least square solution of $y = \mathbf{A}_t \theta_t$:

$$\hat{\theta}_t = \arg\min_{\theta_t} \|y - \mathbf{A}_t \theta_t\| = \left(\mathbf{A}_t^{\Gamma} \mathbf{A}_t\right)^{-1} \mathbf{A}_t^{\Gamma} y$$

(5) Calculate the absolute value of each item of $\hat{\theta}_t$, and select the largest K items. Then the data of $\hat{\theta}_t$ corresponding to each absolute value of the K items is recorded in $\hat{\theta}_{tK}$, the K column vectors in the $\mathbf{A}_t$ correspondingly are marked as $\mathbf{A}_{tK}$, the column serial number of $\mathbf{A}$ are marked as Λ_{tK}. Update the index set $\Lambda_t = \Lambda_{tK}$.

(6) Update residual error:

$$r_t = y - \mathbf{A}_{tK} \hat{\theta}_{tK} = y - \mathbf{A}_{tK} \left(\mathbf{A}_{tK}^{\Gamma} \mathbf{A}\right)^{-1} \mathbf{A}_{tK}^{\Gamma} y.$$

(7) $t = t + 1$, if $t \leq K$, return to step (2) to continue the iteration, otherwise, stop the iteration and proceed to step (8).

(8) Reconstruct the non-zero terms of $\hat{\theta}$ at the index set Λ_{tK} position until the final iteration of $\hat{\theta}_{tK}$.

It is important to note that:

1) In step (3), after solving the set of sequence numbers, make sure that the number of rows of matrix $\mathbf{A}_t$ is not less than the number of columns, which the basis of the least square solution (the columns are linearly independent). If this happens in the first iteration, it means that the algorithm is not suitable for this signal reconstruction.

2) During the iterative process, the set Λ_t in step (3) contains up to $3K$ items (Λ_{t-1} contains K items except for the first iteration, and J_0 contains $2K$ items), step (5) remove at most $2K$ items from Λ_t (remaining K items).

In view of the problem in the model mentioned in section IV part B, the CoSaMP algorithm can solve it effectively. In each iteration, the algorithm first put the $2K$ atoms into the set, and then select the more suitable K atoms. If there are two non-zero terms with the same contribution, using this algorithm, it will not occur to select one atom and weaken the other.

As shown in the simulation of part B of the section IV, when $\left|r_0^{\Gamma} a_{10}\right| = \left|r_0^{\Gamma} a_{13}\right|$ occurs, the 10th and 13th columns of atoms can be recorded in the set at the same time, and the frequencies 593.1Hz and 790.8Hz can be reconstructed to complete the spectrum reconstruction of the original signal.

2) PROBLEMS OF THE MODEL IN THE PROCESS OF RECONSTRUCTION

The CoSaMP algorithm selects multiple atoms in each iteration, which well solves the first case of spectrum division matrix in the discrete multi-coset sampling mathematical model. However, for the second case, the reconstruction failure will be caused by the mutual coherence of the atoms in the compression matrix in the process of reconstruction. When calculating the inner product between the residual vector and the atom in the iterative process, for the frequency with large amplitude, the atom with lager mutual coherence coefficient may increase synchronously or even exceed the atom corresponding to the original non-zero term. In this way, when selecting the multiple atoms, the algorithm may not be able to select effective atoms, resulting in reconstruction failure.

3) SIMULATION ANALYSIS

In the original signal, there are multiple frequencies $f_1 = 115$ Hz and $f_2 = 378.6$ Hz, and their amplitudes are $a_1 = 9.34$ and $a_2 = 5.76$.

The discrete multi-coset sampling frequency is $f = 65.9$ Hz, and the coset number is $p = 4$. During the sampling process, the signal-to-noise ratio of each channel is SNR $= 3$ dB. We set structural parameters $L = 15$ and $c_i = \{0, 2, 5, 11\}$. Then each channel carries out the discrete sampling $N = 102400$ points.

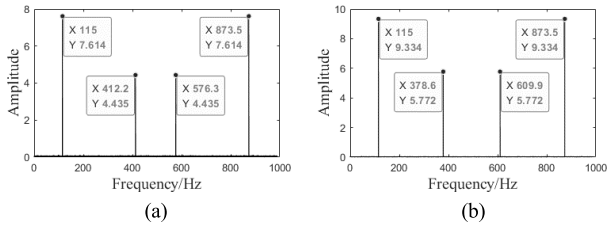

FIGURE 5. (a) is the reconstructed spectrum diagram and (b) is the original signal spectrum diagram.

According to the Fig.3 and the CoSaMP algorithm flow, the spectrum diagram is draw according to the reconstructed spectral value $Y'[k]$, as shown in Fig.5a. The reconstructed frequencies are 115Hz, 412.2Hz, 576.3Hz, and 873.5Hz. In the $\mathbf{Y}'_{\mathrm{L}}$, we have $\mathbf{pos}\left(Y\left[k_{115}\right]\right) = 2$, $\mathbf{pos}\left(Y\left[k_{412.2}\right]\right) = 7$, $\mathbf{pos}\left(Y\left[k_{576.3}\right]\right) = 9$, and $\mathbf{pos}\left(Y\left[k_{875.3}\right]\right) = 14$. From their amplitudes analysis of the reconstruction, the position numbers of $Y\left[k_{115}\right]$ and $Y\left[k_{875.3}\right]$ in the vector satisfy the Eq. (12), $Y\left[k_{412.2}\right]$ and $Y\left[k_{576.3}\right]$ also satisfy it. Only Judging from this result, the signal reconstruction is successful. However, we find that the frequency $f_2 = 378.6$ Hz of the original signal is lost after reconstruction, so it is invalid.

To make a comparison, the Nyquist sampling frequency is $F = Lf = 988.5$ Hz, and the sampling points is $M = NL = 2150400$. We can get the spectral value $Y[k]$ and the spectrum diagram is shown in Fig.5b. The frequency values are 115Hz, 378.6Hz, 609.9Hz, and 873.5Hz. In the $\mathbf{Y}_{\mathrm{L}}$, we have $\mathbf{pos}(Y[k_{115}]) = 2$, $\mathbf{pos}(Y[k_{378.6}]) = 6$, $\mathbf{pos}(Y[k_{609.9}]) = 10$, and $\mathbf{pos}(Y[k_{875.3}]) = 14$. Like the analysis of the reconstructed results of the multi-coset sampling, they also satisfy the Eq. (12).

Compared the two results, it is found that the failure of reconstruction mainly occurs at the frequencies 378.6Hz and 609.9Hz, which move to 412.2Hz and 576.3Hz. There is also a large error in the amplitude of each frequency. This is because $Y\left[k_{115}\right]$ and $Y\left[k_{378.6}\right]$ are in the same column vector Y_{L} ($k_c = 76295$) in the $\mathbf{Y}_{\mathrm{L}}$. When we reconstruct the projection vector Y_{DMCS} ($k_c = 76295$), because of the mutual coherence coefficient $\delta\left(A_{2,9}\right) > \delta\left(A_{2,14}\right) > \delta\left(A_{2,6}\right)$, there will be $\left|r_0^{\Gamma} a_2\right| > \left|r_0^{\Gamma} a_9\right| > \left|r_0^{\Gamma} a_{14}\right| > \left|r_0^{\Gamma} a_6\right|$. According to the steps (2-5) in the algorithm flow, the 9th column atom is identified as the corresponding position of the non-zero term in the sparse vector, and the 6th column atom is ignored. So, the frequency 378.6Hz is reconstructed into 576.3Hz. Similarly, the frequency 609.9Hz becomes onto 412.2Hz.

It can be seen from the algorithm flow that the CoSaMP does not abandon the selected atoms after each iteration. It may cause the same atom to be selected many times because of its large mutual coherence coefficient. The effective atom cannot be selected to make the reconstruction failure.

For the above problems in the model, the reconstruction effect of OMP algorithm is stronger than that of the CoSaMP

algorithm. Because the OMP algorithm selects a single atom at each iteration and discards it after iteration. Such as the example, after the result $|r_0^\Gamma a_2| > |r_0^\Gamma a_9| > |r_0^\Gamma a_{14}| > |r_0^\Gamma a_6|$ appears in the first iteration, the algorithm will select the 2th atom. Then it updates the residual error and discards the 2th atom to continue next iteration. After doing this, it will eliminate the phenomenon that the inner product of the 9th atom is larger because of the higher mutual coherence coefficient.

We use the OMP algorithm to verify. It can reconstruct the frequency of the original signal, and the amplitude error is within the allowable range.

V. THE JOINT OPTIMIZATION ALGORITHM FOR MODEL

A. INTRODUCTION OF ALGORITHM

The signal reconstruction of the discrete multi-coset sampling model is to reconstruct the matrix $\mathbf{Y}_{\mathrm{DMCS}}$ column by column relative to the spectrum division matrix $\mathbf{Y}_{\mathrm{L}}$ to get the reconstructed $\mathbf{Y}'_{\mathrm{L}}$. Different original signals have different frequency relations, so there are different situations in each column vector of $\mathbf{Y}_{\mathrm{L}}$. The single use of OMP or CoSaMP algorithm cannot be applied to the reconstruction of all the column vectors.

From the section IV, we can see that: (1) the CoSaMP algorithm has a good effect on the reconstruction of frequency doubling under the minimum coset number. (2) for the reconstruction effect of the frequency with a specific relationship, the OMP algorithm is better. (3) if a certain frequency is neither double frequency nor a frequency with a specific relationship, the reconstruction process is like the OMP algorithm.

According to the different frequency, the discriminant factor can be introduced when calculating the inner product of the residual vector and the atom, and the reconstruction algorithm is selected reasonably. The process is as follows:

(1) The same initialization.

(2) Calculate the discriminant factor ∇ of the inner product: $\nabla = \left||r_0^\Gamma a_{\lambda_1}| - |r_0^\Gamma a_{\lambda_2}|\right|$, where $\lambda_1 = \arg\max_{1\le j\le L} |r_0^\Gamma a_j|$, $\lambda_2 = \arg\max_{1\le j\le L, j\ne\lambda_1} |r_0^\Gamma a_j|$.

(3) If $\nabla = 0$, selects the CoSaMP algorithm, if $\nabla > 0$, selects the OMP algorithm.

For the spectrum reconstruction of discrete multi-coset sampling model, the OMP algorithm and CoSaMP algorithm can be fused to combine the advantages of the two algorithms under different frequencies to form a joint optimization algorithm for discrete multi-coset sampling (DMCS-DF-JOA). The framework of the system is shown in Fig.6.

B. SIMULATION ANALYSIS

In the original signal, there are multiple frequencies $f_1 = 115$ Hz, $f_2 = 329.5$ Hz, and $f_2 = 378.6$ Hz, and their amplitudes are $a_1 = 9.34$, $a_2 = 7.45$, and $a_3 = 5.76$.

The discrete multi-coset sampling frequency is $f = 65.9$ Hz, and the coset number is $p = 4$. During the sampling process, the signal-to-noise ratio of each channel

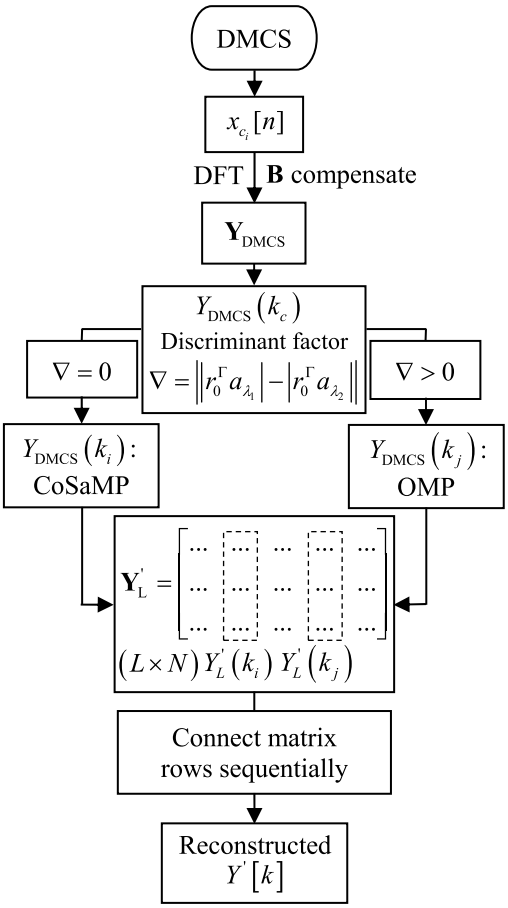

FIGURE 6. Reconstruction system framework diagram of DMCS-DF-JOA.

is SNR = 3 dB. We set structural parameters $L = 15$ and $c_i = \{0, 2, 5, 11\}$. Then each channel carries out the discrete sampling $N = 102400$ points. The OMP algorithm, the CoSaMP algorithm, and the DF-JOA are used to reconstruct the spectrum of the signal, and the results are shown in Fig.7.

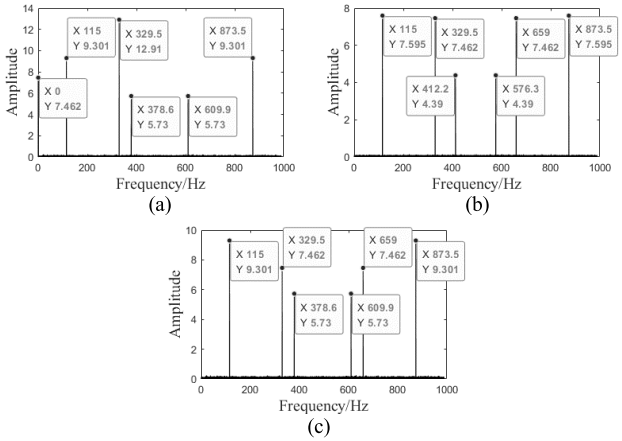

FIGURE 7. (a) is the reconstruction result of the OMP and (b) is the reconstruction result of the CoSaMP and (c) is the reconstruction result of the DF-JOA.

From Fig.7a, the OMP algorithm cannot reconstruct the frequency doubling of the sampling frequency because of the weakening of the atoms with the same contribution. From Fig.7b, the CoSaMP algorithm cannot reconstruct the frequency with a specific relationship because of the influence of the atoms with large mutual coherence coefficient. However, due to the addition of the discriminant factor, the joint optimization algorithm can adaptively recognize the vector features and selects the appropriate algorithm. It accurately reconstructs each frequency and the amplitude error satisfies the allowable range of error, as shown in Fig.7c.

VI. RESEARCH ON JOINT OPTIMIZATION ALGORITHM

A. RELATED DESCRIPTION

Different structural parameters make the characteristics of the compressed matrix **A** different. For all matrices, some may not meet the requirements of compressed matrix mentioned in the part A of section IV.

The main object of this study is the reconstruction algorithm under the minimum coset number, so the structural parameter $p = 4$ is fixed. Different L leads to the different selection of c_i. For discrete sampling of multiple cosets, we default c_1 to 0. That is to say, the first sampling point sampled by Nyquist is taken as the initial sampling point of the first channel. In addition, for the structural characteristics of matrix **A**, if c_1 is not 0, the matrix may not have full rank, which cannot meet the requirements of signal reconstruction. In this way, there are C_{L-1}^{p-1} combinations in the possibility of matrix **A**, and the signal reconstruction success ratio in the case of different **A** is studied.

B. SIMULATION ANALYSIS

Three frequency cases of the original signal: (1) the frequency doubling of the discrete multi-coset sampling frequency (as in part B of section IV). (2) two frequencies that have a specific relationship with the sampling frequency (as in part C of section IV). (3) general frequency without the above two relationships (the two non-zero terms with conjugate relations are in different sparse vectors of the spectrum division matrix, namely the sparsity $K = 1$).

In order to facilitate the subsequent analysis of different frequencies, simulate the discrete multi-coset sampling frequency $f = 65.9$ Hz. Record P_1: $f_1 = 115$ Hz and $f_2 = 378.6$ Hz, the specific relationship is $f_2 = f_1 + 4f$, P_2: general frequency $f_3 = 475.7$ Hz, P_3: doubling frequency $f_4 = 9f = 593.1$ Hz, and the combinations of different conditions.

1) THE INFLUENCE OF FREQUENCEY AMPLITUDE

Considering whether the frequency amplitude affects the reconstruction probability of the signal, simulate three single cases of P_1, P_2, and P_3, and the different combinations between them respectively. The signal-to-noise ratio of each channel is SNR = 3 dB. The total coset number is $L = 21$. Due to the different selection of c_i, there are $C_{L-1}^{p-1} = 1140$ combinations of compressed matrix **A**.

Simulation I: when three kinds of frequency exist alone, OMP algorithm and CoSaMP algorithm are studied, (1) P_1: a_1 varies from 0.5 to 10, $a_2 = 3$. (2) P_2: a_3 varies from 0.5 to 10. (3): a_4 varies from 0.5 to 10. In the case of different compressed matrices, the result of signal reconstruction success ratio is shown in Fig.8a. There is no significant difference between P_2-OMP and P_2-CoSaMP, and both have a high value close to 1. It indicates that the change of amplitude of the general frequency of $K = 1$ has no effect on the reconstruction ratio. There is obvious difference between P_3-OMP and P_3-CoSaMP. The reconstruction effect of CoSaMP algorithm is better than that of OMP, which is consistent with the previous conclusion. The ratio of P_1-OMP and P_1-CoSaMP changes obviously. When the amplitude difference between two frequencies is large, the OMP algorithm is better than the CoSaMP. The amplitude is close to the same so that CoSaMP can select effective atoms, and its effect is better than the that of OMP algorithm.

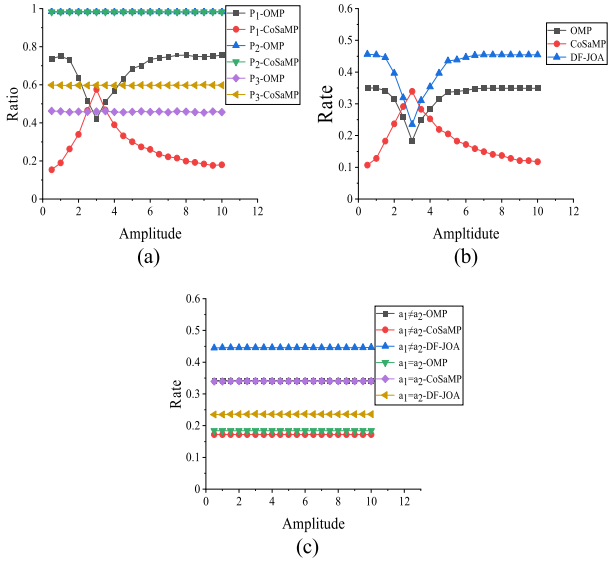

FIGURE 8. (a) is the reconstruction success ratio of simulation I and (b) is the reconstruction success of simulation II and (c) is the reconstruction success of simulation III.

Simulation II: According to the conclusion of simulation I, simulate the existence of three frequencies at the same time. a_1 varies from 0.5 to 10, $a_2 = 3$, $a_3 = 4$, and $a_4 = 10$. Join the research of DF-JOA, and the result is shown in Fig.8b. Due to the complexity of frequency components, the same compressed matrix may satisfy the reconstruction of P_1 but not P_3, so the success ratio of OMP and CoSaMP algorithm are lower than that of Fig.8a. Overall, the joint optimization algorithm with discriminant factor is better than the other two algorithms. Only when the amplitudes of the frequencies of P_1 are close or equal, the CoSaMP rebounds because it directly selects multiple atoms through the calculation of the inner product value. In this case, the effective atoms can

be selected. However, the discriminant factor is very small but not zero, so the OMP is automatically selected for signal reconstruction. After updating the residual, the influence of effective atom is weakened and the success ratio is reduced. This is also a disadvantage of adding the discriminant factor algorithm. The discriminant factor is different because of the different characteristics of the original signal, and there is no absolute limit for selection of the algorithms. Therefore, at present, the discriminant factor $\nabla = 0$ is used to identify the frequency doubling component for signal reconstruction.

Simulation III: The simulation analysis of a_4 is carried out in the two cases of $a_1 \neq a_2$ and $a_1 = a_2$ respectively, and the results are shown in Fig.8c. When $a_1 \neq a_2$, the reconstruction effect of DF-JOA is the best. Due to the influence of the atomic mutual coherence coefficient, when reconstructing P_1, CoSaMP cannot accurately identify effective atoms, which greatly reduces the success ratio. When $a_1 = a_2$, the analysis results of simulation II are confirmed, and the ratio of CoSaMP is higher than that of DF-JOA.

2) THE INFLUENCE OF STRUCTUAL PARAMETER L

When the sampling coset number p is determined, the total coset number L has a certain influence on the structure of the compressed matrix $\mathbf{A}$, the position of non-zero terms in the sparse vector, and the sampling sequence. Therefore, we should consider the influence on the signal reconstruction ratio in the case of different L and how to select the optimal structure parameter to reconstruct the original signal.

In the case of simulating the original with three kinds of frequency situation at the same time, the original signal is sampled by discrete multi-coset sampling by changing the structure parameter L. The original spectrum is reconstructed under different c_i by OMP, CoSaMP, and the DF-JOA.

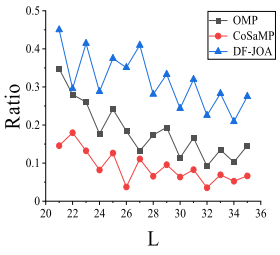

FIGURE 9. Reconstruction success ratio varying with parameter L.

According to the reconstruction results in Fig.9, the ratio of the DF-JOA is higher than that of the other two algorithms. It further proves that the reconstruction effect of the DF-JOA is better than that of the two algorithms with single effect. When the parameter L increases, the reconstruction ratio decreases, but the ratio under odd number is higher than that under even number.

Therefore, after obtaining the range estimation of the maximum frequency of the original signal, we can determine the minimum of the total coset number satisfying the signal reconstruction. The total coset number is preferred to be odd to improve the reconstruction success ratio under different compressed matrices as much as possible.

VII. CONCLUSION

In this article, based on the discrete multi-coset sampling model, we suggest a joint optimization algorithm for identifying multi-band sparse signals, which adapts to the minimum coset number. A signal reconstruction system with discriminant factor is developed to adaptively identify the frequency characteristics and reconstruct the original signal. We do not need to know the support position of the frequency band, but the relevant information about the maximum frequency of the signal.

We discuss the basic knowledge of discrete multi-coset sampling: sampling model, structural parameters, frequency band characteristics, reconstruction requirements and minimum coset number. The compressed matrix of the proposed sampling model has a parameterized structure pattern, which does not have the randomness and independence of the measurement matrix in the traditional compressive sensing.

Our main contribution is to analyze the different characteristics of different frequency components and their relationship with the compressed matrix. In the analysis of frequency doubling of sampling frequency, the OMP algorithm fails to reconstruct because it selects a single atom and ignores the non-zero term with the same contribution. For the frequencies with a specific relationship, the CoSaMP algorithm is affected by the large mutual coherence coefficient of atoms, so when multiple atoms are selected in the iteration, the effective atoms cannot be selected and the sparse vector cannot be reconstructed accurately. According to the advantages and disadvantages of the two algorithms, a joint optimization algorithm with discriminant factor is proposed, which can identify frequency features, automatically select the appropriate reconstruction algorithm, and complete the sparse reconstruction of multi-band signals.

In addition, we also analyze the shortcomings of the parameterized features of the discrete multi-coset sampling compressed matrix and its limitations in sparse reconstruction. Numerical simulation experiments show that the compressed matrix cannot achieve full reconstruction due to the limitation of characteristic, but the joint optimization algorithm can significantly improve the success ratio.

We also get the effect of the frequency amplitude on the success ratio of reconstruction. When the amplitudes of specific relational frequencies are similar, the disadvantages of the joint optimization algorithm are exposed. The discriminant factor introduced in this article can only distinguish between frequency doubling and other frequency components, and cannot accurately identify the differences between different frequencies. The research on this aspect will be carried out in the follow-up, hoping to get a more effective discriminant factor to identify multiple frequencies and achieve a higher success ratio of signal reconstruction.

For the study of the total coset number, the increase reduces the success ratio, but we get that the effect of odd

number is better than that of even number, which can guide us how to better select the structural parameters in the discrete multi-coset sampling.

The research of this article is helpful to collect data when the hardware of discrete multi-coset sampling is limited. We only need the sampling channel with the minimum coset number to complete signal sampling. Then the spectrum characteristics of original signal are obtained under of the condition of sub-Nyquist sampling by the joint optimization algorithm. The research on the better reconstruction algorithm and noise interference in this area will continue to make the sub-Nyquist sampling technology more perfect.

REFERENCES

[1] E. T. Whittaker, "On the functions which are represented by the expansions of the interpolation-theory," *Proc. Roy. Soc. Edinburgh*, vol. 35, pp. 181–194, Jul. 1915.

[2] H. Nyquist, "Certain topics in telegraph transmission theory," *Proc. IEEE*, vol. 47, no. 2, pp. 617–644, Feb. 1928.

[3] V. A. Kotelnikov, "On the transmission capacity of the 'ether' and of cables in electrical communications," in *Proc. 1st All-Union Conf. Technol. Reconstruction Commun. Sector Develop. Low-Current Eng.*, Moscow, Russia, 1933, pp. 1–23.

[4] C. E. Shannon, "Communication in the presence of noise," *Proc. Inst. Radio Eng.*, vol. 37, no. 1, pp. 10–21, Jan. 1949.

[5] A. J. Jerri, "The Shannon sampling theorem—Its various extensions and applications: A tutorial review," *Proc. IEEE*, vol. 65, no. 11, pp. 1565–1596, Nov. 1977.

[6] A. Zayed, *Advances in Shannon's Sampling Theory*. Boca Raton, FL, USA: CRC Press, 1993.

[7] J. R. Higgins, *Sampling Theory in Fourier and Signals Analysis Foundations*. Oxford, U.K.: Oxford Univ. Press, 1996.

[8] M. Mishali, Y. C. Eldar, O. Dounaevsky, and E. Shoshan, "Xampling: Analog to digital at sub-Nyquist rates," *IET Circuits, Devices Syst.*, vol. 5, no. 1, pp. 8–20, Jan. 2011.

[9] H. J. Landau, "Necessary density conditions for sampling and interpolation of certain entire functions," *Acta Mathematica*, vol. 117, no. 1, pp. 37–52, 1967.

[10] A. Papoulis, "Generalized sampling expansion," *IEEE Trans. Circuits Syst.*, vol. 24, no. 11, pp. 652–654, Nov. 1977.

[11] R. Venkataramani and Y. Bresler, "Perfect reconstruction formulas and bounds on aliasing error in sub-Nyquist nonuniform sampling of multiband signals," *IEEE Trans. Inf. Theory*, vol. 46, no. 6, pp. 2173–2183, Sep. 2000.

[12] M. A. Lexa, M. E. Davies, J. S. Thompson, and J. Nikolic, "Compressive power spectral density estimation," in *Proc. IEEE Int. Conf. Acoust., Speech Signal Process. (ICASSP)*, Prague, Czech Republic, May 2011, pp. 3884–3887.

[13] D. D. Arianandа and G. Leus, "Compressive wideband power spectrum estimation," *IEEE Trans. Signal Process.*, vol. 60, no. 9, pp. 4775–4789, Sep. 2012.

[14] D. Cohen and Y. C. Eldar, "Sub-Nyquist sampling for power spectrum sensing in cognitive radios: A unified approach," *IEEE Trans. Signal Process.*, vol. 62, no. 15, pp. 3897–3910, Aug. 2014.

[15] M. Mishali and Y. C. Eldar, "Blind multiband signal reconstruction: Compressed sensing for analog signals," *IEEE Trans. Signal Process.*, vol. 57, no. 3, pp. 993–1009, Mar. 2009.

[16] M. Mishali and Y. C. Eldar, "From theory to practice: Sub-Nyquist sampling of sparse wideband analog signals," *IEEE J. Sel. Topics Signal Process.*, vol. 4, no. 2, pp. 375–391, Apr. 2010.

[17] E. J. Candes, J. Romberg, and T. Tao, "Robust uncertainty principles: Exact signal reconstruction from highly incomplete frequency information," *IEEE Trans. Inf. Theory*, vol. 52, no. 2, pp. 489–509, Feb. 2006.

[18] D. L. Donoho, "Compressed sensing," *IEEE Trans. Inf. Theory*, vol. 52, no. 4, pp. 1289–1306, Apr. 2006.

[19] E. J. Candes and M. B. Wakin, "An introduction to compressive sampling," *IEEE Signal Process. Mag.*, vol. 25, no. 2, pp. 21–30, Mar. 2008.

[20] S. Mallat, *A Wavelet Tour of Signal Processing*. New York, NY, USA: Elsevier, 1999.

[21] R. Baraniuk, "Compressive sensing [lecture notes]," *IEEE Signal Process. Mag.*, vol. 24, no. 4, pp. 118–121, Jul. 2007.

[22] Z. Tian and G. B. Giannakis, "Compressed sensing for wideband cognitive radios," in *Proc. IEEE Int. Conf. Acoust., Speech Signal Process. (ICASSP)*, Honolulu, HI, USA, Apr. 2007, pp. 1357–1360.

[23] M. Fleyer, A. Linden, and M. Horowitz, "Multi-rate synchronous sampling of sparse multi-band signals," *IEEE Trans. Signal Process.*, vol. 58, no. 3, pp. 1144–1156, Mar. 2010.

[24] D. D. Arianandа, G. Leus, and Z. Tian, "Multi-coset sampling for power spectrum blind sensing," in *Proc. IEEE 17th Int. Conf. Digit. Signal Process. (DSP)*, Jul. 2011, pp. 1–8.

[25] C.-P. Yen, Y. Tsai, and X. Wang, "Wideband spectrum sensing based on sub-Nyquist sampling," *IEEE Trans. Signal Process.*, vol. 61, no. 12, pp. 3028–3040, Jun. 2013.

[26] R. Grigoryan, T. Arildsen, D. Tandur, and T. Larsen, "Performance comparison of reconstruction algorithms in discrete blind multi-coset sampling," in *Proc. IEEE Int. Symp. Signal Process. Inf. Technol. (ISSPIT)*, 2012, pp. 147–152.

[27] J. Chen and X. Huo, "Theoretical results on sparse representations of multiple-measurement vectors," *IEEE Trans. Signal Process.*, vol. 54, no. 12, pp. 4634–4643, Dec. 2006.

[28] D. L. Donoho and M. Elad, "Maximal sparsity representation via l_1 minimization," *Proc. Nat. Acad. Sci. USA*, vol. 100, pp. 2197–2202, Mar. 2003.

[29] J. Wen, J. Weng, C. Tong, C. Ren, and Z. Zhou, "Sparse signal recovery with minimization of 1-Norm minus 2-Norm," *IEEE Trans. Veh. Technol.*, vol. 68, no. 7, pp. 6847–6854, Jul. 2019.

[30] D. L. Donoho and M. Elad, "Optimally sparse representation in general (non-orthogonal) dictionaries via minimization," *Proc. Nat. Acad. Sci. USA*, vol. 100, no. 5, pp. 2002–2197, Mar. 2003.

[31] J. Wen, L. Li, X. Tang, and W. H. Mow, "An efficient optimal algorithm for the successive minima problem," *IEEE Trans. Commun.*, vol. 67, no. 2, pp. 1424–1436, Feb. 2019.

[32] J. A. Tropp, "Greed is good: Algorithmic results for sparse approximation," *IEEE Trans. Inf. Theory*, vol. 50, no. 10, pp. 2231–2242, Oct. 2004.

[33] J. A. Tropp and A. C. Gilbert, "Signal recovery from random measurements via orthogonal matching pursuit," *IEEE Trans. Inf. Theory*, vol. 53, no. 12, pp. 4655–4666, Dec. 2007.

[34] H. Li and J. Wen, "Generalized covariance-assisted matching pursuit," *Signal Process.*, vol. 163, pp. 232–237, Oct. 2019.

[35] D. Needell and J. A. Tropp, "CoSaMP: Iterative signal recovery from incomplete and inaccurate samples," *Appl. Comput. Harmon. Anal.*, vol. 26, no. 3, pp. 301–321, May 2009.

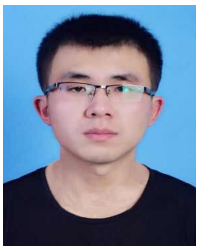

JIANNAN DONG received the B.S. degree in process equipment and control engineering and the M.S. degree in power engineering and engineering thermophysics from Northeast Petroleum University, China, in 2012 and 2017, respectively. He is currently pursuing the Ph.D. degree in mechanical and electronic engineering with the Dalian University of Technology, China. His research interests include compressive sensing and undersampled signal reconstruction.

HONGKUN LI received the B.S., M.S., and Ph.D. degrees from the Dalian University of Technology, China. From 2003 to 2005, he was a Postdoctoral Research Fellow with the Department of Mechanical Engineering, University of Stellard, U.K. He is currently a Professor with the School of Mechanical Engineering, Dalian University of Technology. His research interests include fault diagnosis and operation reliability assessment, weak signal feature information extraction, artificial intelligence, and vibration and noise control.

ZHENFANG FAN received the B.S. degree in mechanical design and manufacturing and automation from Yanshan University, China, in 2017. He is currently pursuing the combined M.S. and Ph.D. degree in mechanical and electronic engineering with the Dalian University of Technology, China. His research interests include undersampling of blade tip timing signal and blade dynamic stress inversion.

QIANG ZHOU received the B.S. degree in mechanical design and manufacturing and automation from Shihezi University, China, in 2015. He is currently pursuing the combined M.S. and Ph.D. degree in mechanical and electronic engineering with the Dalian University of Technology, China. His research interests include fault diagnosis and signal processing of centrifugal pump.

SHUNGANG HUA received the Ph.D. degree in mechanical manufacture and automation from the Dalian University of Technology, China, in 2004. He is currently a Professor with the School of Mechanical Engineering, Dalian University of Technology. His research interests include computer graphics, image processing, and mechanical system dynamics.